Z. Phys. B 97, 139–146 (1995)

ZEITSCHRIFT
FÜR PHYSIK B

Scattering of conduction electrons by surface roughness in thin metal films

A. Kaser, E. Gerlach

VI. Physikalisches Institut, RWTH-Aachen, D-52056 Aachen, Germany

Received: 8 August 1994/Revised version: 16 September 1994

Abstract. A fluctuation transport theory is applied to describe the extra resistivity of thin metal films due to electron scattering at rough surfaces. This scattering mechanism is described in terms of the surface profile autocorrelation. If the lateral extension of the surface structures exceeds the Fermi wavelength, the scattering can be described by a step density of terrace edges.

PACS: 72.10; 73.25; 73.60D

1. Introduction

The resistivity of a metallic conductor can be characterized by a mean free path l_0 of the electrons, which includes elastic and inelastic scattering processes [1]. A scattering-process is called elastic if the scattering-potential is time-dependent (e.g. by ions, surface roughness), otherwise it is called inelastic (e.g. by phonons). If, however, a drifting electron system is considered the scattering-matrix element of an elastic process becomes time-dependent. Here energy is dissipated leading to a relaxation of the Fermi sphere.

If the geometric extension of a specimen exceeds the characteristic transport length l_0, the resistivity can be derived from bulk properties of the material, otherwise surface scattering leads to an important extra resistivity.

In 1938 Fuchs presented an approach to surface scattering in thin metallic films using the Boltzmann theory [2]. Within his framework, the extra resistivity is due to diffuse scattering of conduction electrons at the surface and is described by a phenomenological specularity parameter p. Various scattering mechanisms as by chemisorbed adsorbates or surface roughness were discussed within terms of this parameter [3–5]. Following the concept of diffuse light scattering at rough surfaces Ziman and Soffer established a relation between surface roughness and Fuchs's specularity parameter [8, 9].

Since thin films often have a polycrystalline structure, with a lateral extension of the crystallites comparable to the film thickness [10], we have to distinguish between a macroscopic roughness, given by crystallite height fluctuations, and a microscopic one which originates from height fluctuations on an atomic scale.

A measurement of the resistance during the growth of an ad-layer allows to determine the change of the resistivity as a function of the changing surface morphology. This differential method eliminates the effect of unknown scattering-mechanisms, e.g. by inner grain boundaries of the substrate. Depending on the growth conditions the variation of the morphology can be chosen to reach from atomic roughness (coverage by less than a monolayer) up the region of deep roughness.

In the present paper we treat the electron scattering in noble metals by surface roughness in a quantum mechanical context which is based on a fluctuation concept [11–16]. The autocorrelation of the surface morphology plays a major role for the resulting extra resistivity. It is discussed for several autocorrelation functions, describing atomic roughness including island-like growth and the regime of high coverage. We assume the autocorrelation function to consist of two independent parameters, the vertical mean square roughness Δ^2 and the correlation length ξ which characterizes the lateral homogenity of the surface. Considering only the influence of Δ^2 yields a parabolic dependence of the extra resistivity on the monolayer coverage during the growth of the first adlayer, in this context called Nordheim behaviour. The lateral correlation length ξ is responsible for an interesting and characteristic deviation from the parabolic behaviour. Our results are shown to be in good agreement with the experimental ones referenced in [5, 20, 19].

2. Theoretical concept

We consider a thin film laterally extended in the $\boldsymbol{r} = (x, y)$ directions and confined in z-direction to $0 < z < d$ as a model system for a particular crystallite of the substrate, where d is the average film thickness, A the film area and n_e the three dimensional electron density, see Fig. 1.

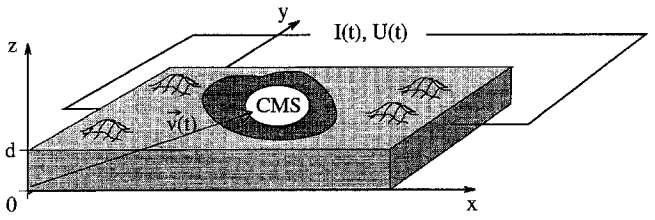

Fig. 1. The current transport in a film of thickness d can be represented by the center of mass system of the electron which moves with a velocity $v(t)$. The dents indicate the surface roughness

The band structure of noble metals projected onto the surface orientation often has an energy gap at the Fermi energy in the Γ point of the Brillouin zone [6]. These electrons cannot travel perpendicularly to the surface and, thus, are not scattered by the surface roughness. However, Sambles has shown that for the (111) surface orientation, considered in the present paper, this effect is negligible [7]. For this reason the electrons will be treated as a free electron gas.

When the electrons are scattered by the surface, they feel only potential variations due to the spatially outermost electron density, which shows nearly no corrugation in the case of smooth surfaces. Therefore, the crystal structure is of negligible importance for the mechanism of specular reflection and, thus, we are allowed to describe an ideal surface within a jellium model. Deviations from the smooth surface at $z = d$ are now described by local broadening $\Delta(\boldsymbol{r})$ of the confining potential. If the electrons in the smooth film are confined by the potential $V_0(z)$, the rough film can be described by the new potential [17]

$$V(\boldsymbol{r},z) = V_0\left(z\cdot\frac{d}{\Delta(\boldsymbol{r})+d}\right) \approx V_0(z) - z\cdot\frac{\Delta(\boldsymbol{r})}{d}\,V_0'(z). \tag{1}$$

This leads to the one particle Hamiltonian for free electrons, confined in z-direction, with the scattering potential $\phi(\boldsymbol{r},z)$

$$H = \frac{p^2}{2m} + V_0(z) + \phi(\boldsymbol{r},z) \quad \phi(\boldsymbol{r},z) = -z\cdot\frac{\Delta(\boldsymbol{r})}{d}\,V_0'(z) \tag{2}$$

with the eigenfunctions $\Phi_{k,n}(\boldsymbol{r},z)$ and eigenvalues $W_{k,n}$ of the unperturbed Hamiltonian:

$$\Phi_{k,n}(\boldsymbol{r},z) = \frac{1}{\sqrt{A}}\exp(i\boldsymbol{k}\cdot\boldsymbol{r})\cdot\varphi_n(z). \tag{3}$$

The polarizability Π of the corresponding non-interacting unperturbed many particle system is given by [18]:

$$\Pi(\boldsymbol{k},\omega,z,z') = \sum_{n,m}\Pi_{n,m}(\boldsymbol{k},\omega)\cdot\varphi_n(z)\varphi_n(z')\varphi_m(z)\varphi_m(z') \tag{4}$$

with

$$\Pi_{n,m}(\boldsymbol{k},\omega) = \frac{2}{A}\sum_{q}\left\{\frac{f(W_{q,n})}{\hbar\omega + i\hbar 0_+ + W_{q,n} - W_{q+k,m}} - \frac{f(W_{q,n})}{\hbar\omega + i\hbar 0_+ + W_{q+k,m} - W_{q,n}}\right\}.$$

We now apply the fluctuation transport concept to the present problem, where we in general assume on oscillating external field $\boldsymbol{E}_{\text{ext}}(\Omega)$. Later in the application we confine our attention to dc-transport. The fluctuation concept uses the assumption that all electrons contribute to the macroscopic current density $\boldsymbol{j} = -en_e\boldsymbol{v}_d$ with the same drift-velocity $\boldsymbol{v}_d$, n_e the three dimensional electron density. Thus, the motion of the carrier system is divided into a collective drift $\boldsymbol{v}_d$ of their center of mass system (CMS) and a disordered thermal motion. The stationary transport is characterized by a macroscopic force-density balance that takes friction-forces, inertia and driving forces into account:

$$\boldsymbol{f}(\boldsymbol{v}_d) - mn_e\dot{\boldsymbol{v}}_d - en_e\boldsymbol{E}_{\text{ext}} = 0, \tag{5}$$

$$\boldsymbol{j} = -en_e\boldsymbol{v}_d = \boldsymbol{\sigma}\boldsymbol{E}_{\text{ext}}. \tag{6}$$

In the linear regime we expect the friction to be proportional to the velocity. Defining the friction coefficient γ by $\boldsymbol{f}(\boldsymbol{v}_d) = -\gamma\cdot\boldsymbol{v}_d$ Fourier transformation of (5) and (6) gives the frequency dependent resistivity tensor:

$$\boldsymbol{\rho}(\omega) = \frac{1}{n_e^2e^2}\,\gamma(\omega) - i\,\frac{m\omega}{n_ee^2}\,\boldsymbol{1}. \tag{7}$$

The friction-forces will now be derived from a microscopic treatment of the scattering mechanisms.

The fluctuations of the scattering potential in our system leads to an induced carrier density ϱ_i and a corresponding electric field $\boldsymbol{E}_i$, which gives rise to an energy dissipation of the drifting electron system. This dissipative process can be described in terms of a friction-force $\boldsymbol{f}(\boldsymbol{v}_d)$:

$$\boldsymbol{f}(\boldsymbol{v}_d) = \frac{1}{Ad}\left\langle\int\varrho_i(\boldsymbol{r},z,t)\boldsymbol{E}_i(\boldsymbol{r},z,t)\,\mathrm{d}\boldsymbol{r}\mathrm{d}z\right\rangle_{\text{ens}}, \tag{8}$$

where the ensemble average is taken over all configurations of the statistically distributed scattering potentials (e.g. of the roughness).

It s convenient to calculate the induced carrier density ϱ_i in their own rest system ($\boldsymbol{v}_d = 0$), because therein the bilocal polarizability $\Pi(\boldsymbol{k},\omega,z,z')$ of a non-interacting electron gas is well-known [18]. The screening of the scattering potential ϕ is handled within the random-phase approximation, which corresponds to a self-consistence step in the calculation of the induced charge density in our approach and results in an effective potential ϕ_{eff}.

The motion of the electrons in the center of mass system (CMS) relative to the resting crystal system (LS) is given by $\boldsymbol{R}(t) = \boldsymbol{R}_0\sin(\Omega t)$, which means a time dependent drift-velocity $\boldsymbol{v}_d$. The Fourier components of a scalar operator $B(\boldsymbol{r},z,t)$ are then transformed by means of a Doppler-type frequency shift:

$$B_{\text{LS}}(\boldsymbol{k},z,\omega) = B^{\text{CMS}}(\boldsymbol{k},z,\omega) + \alpha(\boldsymbol{k})B^{\text{CMS}}(\boldsymbol{k},z,\omega-\Omega)$$

$$\alpha(\boldsymbol{k}) = \frac{\boldsymbol{k}\cdot\boldsymbol{R}_0}{2}, \tag{10}$$

where the upper index (CMS) indicates that the operator is described in the rest system of the carriers and the lower index (LS) means the same operator in the crystal system.

Typical drift velocities $\boldsymbol{R}_0 \cdot \Omega$ of metal electrons are of the order of cm/s ($\ll v_f$) and, thus, a first order calculation in α is a good approximation.

In the following discussion we write down only the Fourier components including '$-\Omega$' and omit wave-vector arguments where it is unambiguous.

The effective potential ϕ_{eff} felt by the electrons consists of two contributions, on one hand of the unscreened potential ϕ, and on the other hand of the induced potential $\delta\phi_i$ due to the induced charge density. These quantities have to be calculated self-consistently:

$$\varrho_i(\omega, z) = \varrho^i(\omega, z) + \alpha\varrho^i(\omega - \Omega), \tag{11}$$

$$\varrho^i(\omega, z) = q\int \Pi(\omega, z, z')\phi^{\text{eff}}(\omega, z')\,\mathrm{d}z', \tag{12}$$

$$\phi_{\text{eff}}(\omega, z) = \phi(\omega, z) + \delta\phi_i(\omega, z), \tag{13}$$

$$\delta\phi_i(\omega, z) = \frac{q}{2\varepsilon_0 k}\int \exp(-k|z - z'|)\varrho_i(\omega, z')\,\mathrm{d}z', \tag{14}$$

$$\begin{aligned}\varrho_i(\omega, z) = {} & q\int \Pi(\omega, z, z')\phi_{\text{eff}}(\omega, z')\,\mathrm{d}z' \\ & - \alpha q\int (\Pi(\omega, z, z') \\ & - \Pi(\omega - \Omega, z, z'))\phi_{\text{eff}}(\omega - \Omega, z')\,\mathrm{d}z',\end{aligned} \tag{15}$$

q is the charge of the carriers. Introducing the dielectric function $S(\boldsymbol{k}, \omega, z, z')$ the problem can be rewritten as an integral equation for the effective potential:

$$\begin{aligned}\phi_{\text{eff}}(\omega, z) = {} & \phi(\omega, z) - \int \chi(\omega, z, z')\phi_{\text{eff}}(\omega, z')\,\mathrm{d}z' \\ & - \alpha\int (S(\omega - \Omega, z, z') \\ & - S(\omega, z, z'))\phi_{\text{eff}}(\omega - \Omega, z')\,\mathrm{d}z',\end{aligned} \tag{16}$$

$$\chi(\omega, z, z') = -\frac{q^2}{2\varepsilon_0 k}\int \exp(-k|z - z''|)\Pi(\omega, z'', z')\,\mathrm{d}z'', \tag{17}$$

$$S(\omega, z, z') = \delta(z - z') + \chi(\omega, z, z'). \tag{18}$$

The inverse dielectric function $S^{-1}(\omega, z, z')$ is defined by the aid of the unity operator $\delta(z - z')$ in the space of functions. Equation (16) can be solved by iteration up to first order in $\alpha(\boldsymbol{k})$:

$$\delta(z - z') = \int S^{-1}(\omega, z, z'')S(\omega, z'', z')\,\mathrm{d}z'', \tag{19}$$

$$\begin{aligned}\phi_{\text{eff}}(\omega, z) = {} & \int S^{-1}(\omega, z, z')\phi(\omega, z')\,\mathrm{d}z' \\ & - \alpha\int (S^{-1}(\omega, z, z') \\ & - S^{-1}(\omega - \Omega, z, z'))\phi(\omega - \Omega, z')\,\mathrm{d}z',\end{aligned} \tag{20}$$

$$\begin{aligned}\varrho_i(\omega, z) = {} & q\int \Pi(\omega, z, z')S^{-1}(\omega, z', z'')\phi(\omega, z'')\,\mathrm{d}z'\mathrm{d}z'' \\ & - \alpha q\int \Pi(\omega, z, z')S^{-1}(\omega, z', z'') \\ & \times \phi(\omega - \Omega, z'')\,\mathrm{d}z'\mathrm{d}z'' \\ & + \alpha q\int \Pi(\omega - \Omega, z, z')S^{-1}(\omega - \Omega, z', z'') \\ & \times \phi(\omega - \Omega, z'')\,\mathrm{d}z'\mathrm{d}z''.\end{aligned} \tag{21}$$

In order to calculate the friction force we insert (21) into (8). Under the assumption of a radially symmetric autocorrelation function of the surface profile, a box potential with barrier height V_0 and a current in x-direction, we obtain the following expression for the extra resistivity due to surface roughness scattering:

$$\rho(\omega) = \frac{\gamma(\omega)}{n_e^2 q^2} - i\frac{m\omega}{nq^2}, \tag{22}$$

with

$$\begin{aligned}\gamma(\omega) = {} & \frac{i}{(2\pi)^2\,\mathrm{d}\omega}\int \mathrm{d}\boldsymbol{k}\,\mathrm{d}z\,\mathrm{d}z_1\,k_x^2 V_0^2 K(\boldsymbol{k}) \\ & \times (\Pi(\boldsymbol{k}, \omega, z, z_1)S^{-1}(\boldsymbol{k}, \omega, z_1, d)S^{-1}(-\boldsymbol{k}, 0, z, d) \\ & - \Pi(\boldsymbol{k}, 0, z, z_1)S^{-1}(\boldsymbol{k}, 0, z_1, d)S^{-1}(-\boldsymbol{k}, \omega, z, d))\end{aligned} \tag{23}$$

and

$$K(k) = \frac{1}{A}|\Delta(k)|^2. \tag{24}$$

$K(k)$ is the power spectrum of the Fourier transformed surface profile function.

Since the resistivity of metals is practically frequency-independent up to the plasma resonance frequency we will restrict ourselves to dc-transport properties. Furthermore we will discuss only the non-quantized regime, which means a dense subband structure in the limit $k_f d \to \infty$. For this case we expect a geometric behaviour $\gamma \propto 1/d$ of the friction coefficient which is due to the ratio of surface area to volume. For a workfunction Φ_a of the order of the Fermi energy W_f, it can be shown that an infinitely high barrier $V_0 \to \infty$ yields the leading order $1/d$ of the resistivity. The remaining problem is the inversion of the dielectric tensor $S(k, 0, z, z')$ at frequency zero, which is analytically possible only for systems with one occupied subband or translationally invariant systems.

Here we only give a rough estimate of the inversion of $S(0, z, z')$ which is similar to the Fermi-Thomas method in three dimensions [1]. Within this approximation the polarizability Π is projected onto the diagonal in the coordinate space,

$$\begin{aligned}\Pi(k, 0, z, z') \to {} & \int \Pi(k, 0, z, z'')\,\mathrm{d}z'' \\ & \cdot \delta(z - z') = -\frac{\varepsilon_0 k_{\text{FT}}^2}{q^2} f(k, z) \cdot \delta(z - z'),\end{aligned} \tag{25}$$

so that the dielectric tensor can be written as:

$$S(k, 0, z, z') = \delta(z - z') + \frac{k_{\text{FT}}^2}{2k}\exp(-k|z - z'|)f(k, z'), \tag{26}$$

k_{FT} the Fermi-Thomas wavelength of the three dimensional-theory. The function $f(k, z)$ is approximated by interpolating between the limits $k/k_f \ll 0$ and $k/k_f \gg 1$ of the polarizability Π:

$$f(k, z) = \left(\frac{\pi}{3n_{el}}\right)^{1/3}\sum_{n \le n_f}\frac{k_f^2(n)}{k^2/2 + k_f^2(n)}\,\varphi_n^2(z). \tag{27}$$

The ansatz

$$S^{-1}(k,0,z,z') = \delta(z-z') - \frac{k_{FT}^2}{2k} f(k,z')s(z,z') \tag{28}$$

leads to the integral equation for the unknown function $s(z,z')$

$$s(z,z') = \exp(-k|z-z'|) - \frac{k_{FT}^2}{2k} \times \int_0^d s(z,z'')f(k,z'')\exp(-k|z''-z'|)\,dz''$$

which can be solved analytically if we approximate the spatially smooth function $f(k,z)$ by its average value $f(k)$.

Inserting the inverse dielectric function (28) in (23) and transforming the summation over the subband indices (originating from the polarizability Eq. 4 and 23) into integrals we obtain the following result for the extra resistivity $\Delta\rho$:

$$\Delta\rho = \frac{9\hbar}{2dq^2} k_f^2 \int_0^1 dx \int_0^1 dy \int_0^\pi d\Theta \int_0^{2\pi} d\varphi \times \frac{\cos^2(\varphi)}{\pi} k^2(x,y,\Theta) \cdot \left\{ xy - \frac{1}{3} g(k(x,y,\Theta)) H\left(x,y,\frac{k(x,y,\Theta)}{\sqrt{2}}, \frac{k_{FT}}{2k_f}\right)\right\}^2 \cdot K(k_f\sqrt{2}k(x,y,\Theta)\cos(\varphi), k_f\sqrt{2}k(x,y,\Theta)\sin(\varphi)) \tag{29}$$

with

$$k(x,y,\Theta) = \left\{\sqrt{1-x^2}\sqrt{1-y^2}\cos(\Theta) + \frac{2-x^2-y^2}{2}\right\}^{1/2},$$

$$g(x) = 1 - \frac{x^2}{3} - \frac{x^2 \operatorname{atanh}(1/\sqrt{x^2+1}) + x^4 \operatorname{atanh}(1/\sqrt{x^2+1})}{3\sqrt{x^2+1}}, \tag{30}$$

$$H(x,y,z,\delta) = \frac{1}{(z^2 + \delta^2 f_\infty(\sqrt{2}z) + (x-y)^2/4)} \cdot \frac{1}{(z^2 + \delta^2 f_\infty(\sqrt{2}z) + (x+y)^2/4)} \times \frac{\delta^2 xy}{1 + z/\sqrt{z^2 + \delta^2 f_\infty(\sqrt{2}z)}},$$

$$f_\infty(x) = 1 - x^2 \frac{\operatorname{atanh}(1/\sqrt{x^2+1})}{\sqrt{x^2+1}}. \tag{31}$$

In the next section we discuss formula (29) for several autocorrelation functions which describe various surface formations.

3. Model systems

The effect of surface roughness on metal film resistivity will be discussed for two model systems characterized by different profile autocorrelations.

The first model deals with a smooth substrate film covered by less than a monolayer, coverage $\Theta \ll 1$, of the same material, for instance Ag on Ag(111). This description includes isolated ad-atoms and laterally extended conglomerates. The morphology will be characterized by an atomic form factor and a structure factor which is given by the arrangement of the ad-atoms.

The second model is for surfaces that cannot be divided into topological subregions. This description holds for surfaces with profile height variations of more than a monolayer. This we call the regime of "high roughness". Since in the framework of "low coverage" some results from the "high roughness" regime are needed, we will discuss the latter first.

3.1. High roughness

The autocorrelation $K(r)$ of the surface profile on one hand gives the lateral length scale ξ of the self-similarity of the profiles and on the other hand a vertical scale which is called the mean square roughness Δ^2. Both length scales are independent of each other.

As model functions we consider a Gaussian, a Lorentzian, and an exponential decay profile. For the extra resistivity $\Delta\rho$ we obtain the simple formulas:

$$\Delta\rho = \frac{9\hbar\Delta^2}{2q^2 d} \cdot \begin{cases} G\left(\xi k_f, \frac{k_{FT}}{2k_f}\right) & \text{if } K(r) = \Delta^2 \exp(-(r/\xi)^2), \\ E\left(\xi k_f, \frac{k_{FT}}{2k_f}\right) & \text{if } K(r) = \Delta^2 \exp(-(r/\xi), \\ L\left(\xi k_f, \frac{k_{FT}}{2k_f}\right) & \text{if } K(r) = \Delta^2 \frac{\xi^2}{\xi^2 + r^2}. \end{cases} \tag{32}$$

The functions G, E, L are shown in Figs. 2 to 4. As is known from wave scattering theory the diffraction is most efficient if the particles wavelength $\propto k_f^{-1}$ is of the order of the extension of the obstacles. Thus the resistivity has a maximum for $\xi k_f \approx 2$ which is nearly independent of the choice of the special autocorrelation.

Comparing our results with Fuchs's theory, we can interpret the functions G, E, L as a measure for the amount of diffusely reflected electrons, for example with exponential decay:

$$\left.\frac{\Delta\rho}{\rho_0}\right|_{\text{Fuchs}} = \frac{3l}{8d}(1-p), \quad l = v_f\tau, \tag{33}$$

$$(1-p) = \frac{4(\Delta k_f)^2}{\pi^2} E\left(\xi k_f, \frac{k_{FT}}{2k_f}\right). \tag{34}$$

Here we calculated the phenomenological specularity parameter p on a quantum mechanical basis. Depending on the explicit surface profile the right hand side of (34)

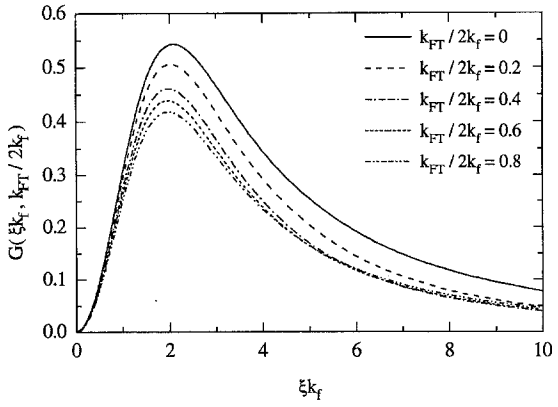

Fig. 2. Scattering contribution G for a Gaussian profile as a function of ξk_f for various screening parameters $k_{FT}/2k_f$ (0.75 for Ag). Surface structures with a characteristic lateral extension ξ of the same length as the Fermi wavelength are the most efficient scatterers

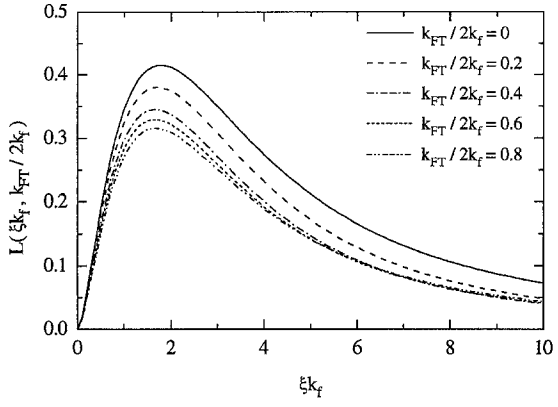

Fig. 3. Scattering contribution L for a Lorentzian profile as a function of ξk_f for various screening parameters $k_{FT}/2k_f$

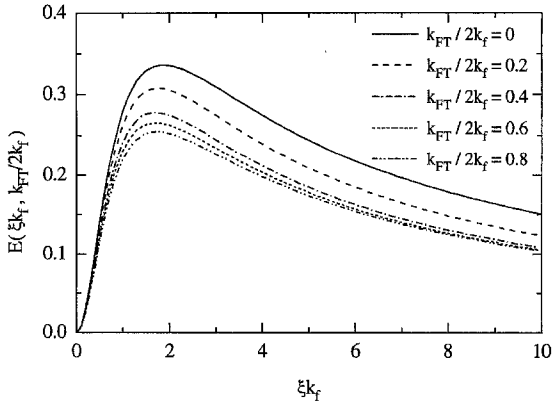

Fig. 4. Scattering contribution E for an exponential decaying correlation function

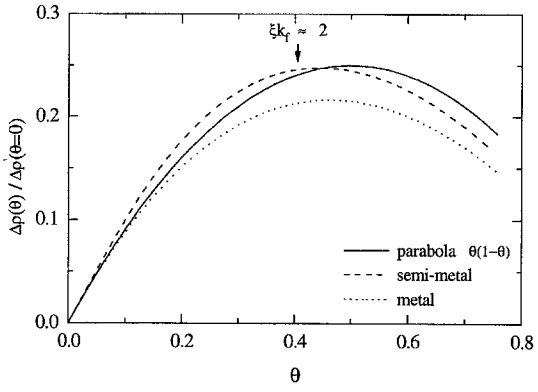

Fig. 5. Schematic deviations of the resistivity from the Nordheim behaviour (parabola) during the growth of the first monolayer on an atomic smooth substrate film for metals and semi-metals. The increase of resistivity is normalized to the initial slope $\rho' = \partial/\partial\Theta\,\Delta\rho$ at $\Theta = 0$. The deviations result from the monolayer coverage dependence (Θ) on the product ξk_f

can become larger than 1, this region exceeds the validity of Fuchs's formula.

We should remark that in (34) the characteristic lateral and vertical lengths (ξ, Δ^2) scale with the wavelengths of the particles, which leads to an interesting behaviour during the growth of the first ad-layer.

If the material grows layer by layer, as In on In (111) [5], the vertical roughness shows a parabolic dependence on the coverage known as Nordheim behaviour: $\Delta^2 = a^2\Theta\cdot(1-\Theta)$, where a is the distance between two layers in the growth direction. If we neglect the effect of the correlation lengths ξ we would expect the same dependence for the extra resistivity.

For $\Theta \ll 1$ the ad-atoms are isolated and the corresponding correlation length ξ is of the order of an atomic radius. With increasing coverage the lateral extension of the structures and in the same way ξ will increase.

In metal films the de-Broglie wavelength of the electrons is of the order of atomic distances and thus the product ξk_f will be larger than 2 and increase further during the growth of the film. As a consequence the scattering efficiency decreases and the observed resistivity lies below the parabolic behaviour as is shown in Fig. 5. This behaviour has been observed experimentally for In on In(111) [5].

Since in semi-metals the electron de-Broglie wavelength is larger than the interatomic distances, the product ξk_f is smaller than 2 for the region of isolated ad-atoms. In this case an increasing correlation length leads to an increase of the diffusely scattered electrons until the value $\xi k_f = 2$ will be passed. Then the resistivity behaves as in the case of metals, see Fig. 5. It is an interesting question whether this deviation from the Nordheim behaviour can be observed experimentally.

A priori it is not clear which of our correlation functions holds to describe a real surface profile. Henzler and Luo [19] observed the growth of silver films by high resolution Spot Profile Analysis LEED and compared this results with simultaneous resistivity measurements. From comparison with our theoretical approach the exponential decay appears to be the best description. This is in agreement with our results of a growth simulation in which we calculated the phase-correlation, responsible for the SPA-LEED signal, and the autocorrelation function. More details will be published elsewhere.

3.2. Low coverage

Within our jellium model the electron density at a smooth surface is constant in lateral direction. An adsorbed ad-atom distorts the planes of constant density and thus can be described by a dent $f(\boldsymbol{r})$, see Fig. 6. If there are N of such ad-atoms the new topology $\Delta(\boldsymbol{r})$ is given by a statistic ensemble $\{\boldsymbol{r}_i\}$ over all ad-atom positions. $K(\boldsymbol{k})$ is the corresponding autocorrelation in Fourier space:

$$\Delta(\boldsymbol{r}) = \sum_{i=1}^{N} f(\boldsymbol{r} - \boldsymbol{r}_i), \tag{35}$$

$$K(\boldsymbol{k}) = \frac{N}{A} |f(\boldsymbol{k})|^2 \left\langle \frac{1}{N} \sum_{L,j} \exp(-i\boldsymbol{k} \cdot (\boldsymbol{r}_i - \boldsymbol{r}_j)) \right\rangle. \tag{36}$$

The form of the dent is chosen to be Gaussian. This guarantees that the surface profile variation is concentrated to the vicinity of the ad-atom position and has the advantage of a simple analytical Fourier transform. The amplitude is given by the distance a of two net-planes, the width is fitted to the volume of an atom in the crystal lattice:

$$f(r) = \Delta \exp(-(r/r_0)^2), \quad \pi r_0^2 = (\Delta n_{at})^{-1}. \tag{37}$$

The topological arrangement is represented by a set $\{L\}$ of conglomerates with a set of inner ad-atoms positions $\{\boldsymbol{r}_{i,L}\}$, Fig. 7.

Due to to the polycrystalline structure of the substrate film we do not expect a preferred orientation of the clusters and carry out an angle average over the connection vectors of two ad-atoms in the vector product $\boldsymbol{k} \cdot (\boldsymbol{r}_{i,L} - \boldsymbol{r}_{j,M})$. In this way we obtain an autocorrelation with an effective structure factor $\Gamma(k)$:

$$K(k) = \frac{N}{A} |f(k)|^2 \Gamma(k), \tag{38}$$

$$\Gamma(k) = 1 + \frac{2}{N} \left\langle \sum_{L, j_L < i_L} \mathrm{J}_0(k|\boldsymbol{r}_{i_L} - \boldsymbol{r}_{j_L}|) \right\rangle + \frac{2}{N} \left\langle \sum_{L<M, i_L, j_M} \mathrm{J}_0(k|\boldsymbol{r}_{i_L} - \boldsymbol{r}_{j_M}|) \right\rangle. \tag{39}$$

The first term of Γ is due to scattering at single ad-atoms, the second one gives the correction due to formation of conglomerates. The third term gives the correlation between two different conglomerates and will be neglected in the following discussion.

In a first step we calculate the initial slope of the extra resistivity as a function of the monolayer coverage Θ, since this slope is characteristic for the uncorrelated region and therefore typical for the material under consideration. From (29) we find

$$\left.\frac{\partial}{\partial \Theta} \Delta\rho\right|_{\Theta=0} = \frac{9\hbar}{2dq^2} k_f^2 \int_0^1 \mathrm{d}x \int_0^1 \mathrm{d}y \int_0^{\pi} \mathrm{d}z\, k^2(x,y,z) \cdot \left\{ xy - \frac{1}{3} g(k(x,y,z)) H\left(x, y, \frac{k(x,y,z)}{\sqrt{2}}, \frac{k_{\mathrm{FT}}}{2k_f}\right)\right\}^2 \cdot \pi \Delta^2 r_0^2 \exp(-(k_f r_0 k(x,y,z))^2) \times \Gamma(\sqrt{2} k_f k(x,y,z)). \tag{40}$$

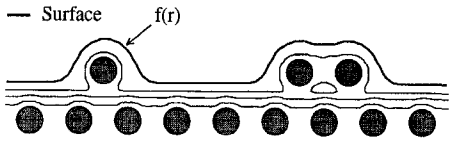

Fig. 6. Within the jellium model the shift of the contours of constant electron density due to ad-atoms is described by a broadening $\Delta(r)$ of the confining potential $V_0(z)$ by $\Delta(r)$. $\Delta(r)$ is the sum of the single atom factors $f(r)$

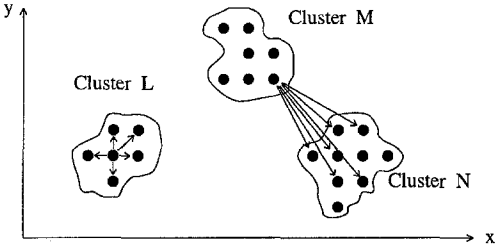

Fig. 7. Division of the ad-atoms arrangement into topological subgroups. Each arrow represents the interaction between different ad-atoms

In the uncorrelated limit we must put $\Gamma = 1$, and (40) reduces to:

$$\left.\frac{\partial}{\partial \Theta} \Delta\rho\right|_{\Theta=0} = \frac{9\hbar}{2dq^2} \frac{\Delta^2}{2} G\left(\sqrt{2} r_0 k_f, \frac{k_{\mathrm{FT}}}{2k_f}\right), \tag{41}$$

with G from Fig. 2. Table 1 shows good agreement between the experimental and theoretical results for several materials.

In a second step we consider the effect of accumulated ad-atoms. As an example we present the results for circular conglomerates consisting of M ad-atoms leading to a radius $R_M = r_0 \cdot \sqrt{M}$. For this arrangement we have to calculate the structure factor Γ in (40).

If the electrons wavelength does not resolve the atomic separations the summation over the ad-atom positions $\{\boldsymbol{r}_{i,M}\}$ in (39) can be approximated by integrals over the conglomerate area:

$$\Gamma(k) = MF(kr_0\sqrt{M}) \quad F(x) = 2\int_0^2 \mathrm{d}z f(z) J_0(xz), \tag{42}$$

$$f(z) = \begin{cases} z(1-z)^2 \hat{H}(1-z) \\ \quad + \dfrac{2\pi}{\pi} \displaystyle\int_{|1-z|}^{1} \mathrm{d}t \arccos\left(\frac{z^2 + t^2 - 1}{2zt}\right), \\ 0 \quad z \notin [0,2] \quad \hat{H}(z<0) = 0 \end{cases} \tag{43}$$

$\hat{H}(z)$ the Heavyside function.

We discuss the effect of formation of conglomerates by introducing a scattering efficiency η, that is the ratio of extra resistivity with and without (i.e. independent ad-atoms) clusters:

$$\eta = \frac{\Delta\rho(M)}{\Delta\rho(1)}, \tag{44}$$

Table 1. Comparison of the experimentally investigated values for the initial slope of the resistivity change $\partial/\partial\Theta\,\Delta\rho|_{\Theta=0}$ with the theoretical results. a the lattice constant, d thickness of the substrate film, ML monolayer. Data are taken from [5] (Ag, Cu) and [20]

System	a[Å]	k_f[Å^{-1}]	d[Å]	exp. [$\mu\Omega$cm/ML]	theor. [$\mu\Omega$cm/ML]
Cu on Cu (111)	3.61	1.36	220	0.6 ± 0.2	0.73
Ag on Ag (111)	4.09	1.20	200	1.3 ± 0.1	1.05
Au on Au (111)	4.08	1.20	220	1.1 ± 0.1	0.95

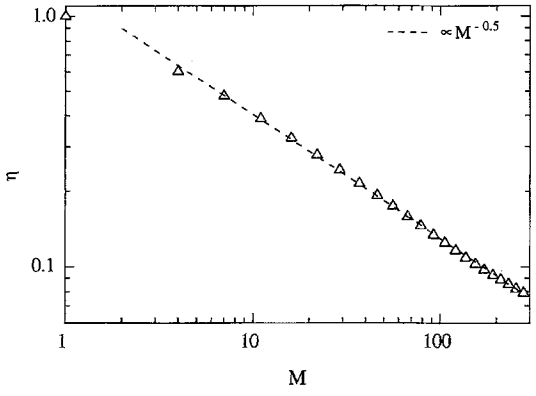

Fig. 8. Scattering efficiency η as a function of atoms per cluster M for a metallic system characterized by $k_f r_0 \approx 1.7$ and $k_{FT}/2k_f = 0.75$. Due to the small Fermi wavelength the electrons are only scattered at the edges of the conglomerates, which corresponds to a decreasing efficiency $\eta \propto M^{-0.5}$

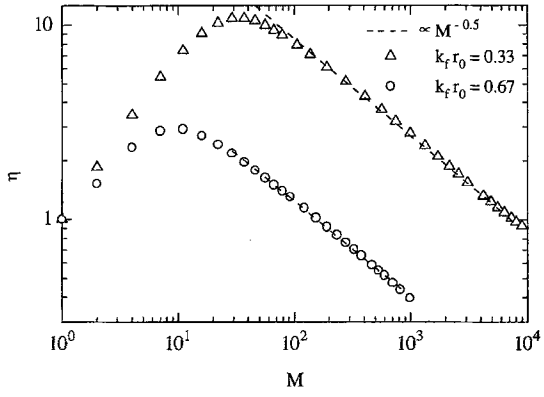

Fig. 9. Scattering efficiency η as a function of atoms per cluster M for semi-metals characterized by $k_f r_0 = 0.33$ and $k_f r_0 = 0.67$. Since the Fermi wavelength of the electrons is larger than the interatomic distances, the formation of conglomerates leads to an increasing efficiency until the lateral extension R_M of the clusters becomes so large that $k_f R_M$ is larger than 2. Then the system shows metallic behaviour with decreasing efficiency

the total density of atoms is taken to be constant. The calculations of the efficiency were done for metals and semi-metals.

In the calculations we put the screening parameter for metals to be $k_{FT}/2k_f = 0.75$ whereas for semi-metals we took $k_{FT}/2k_f \ll 1$ because of the high dielectric constant of the lattice. Furthermore we chose $k_f r_0 \approx 1.75$ which is typical for a cubic crystal structure and $k_f r_0 = 0.33, 0.67$ as examples for semi-metals.

Figure 8 shows the scattering efficiency for metals as a function of atoms per cluster. Since the electron de-Broglie wavelengths in metals are of the order of the inter-atomic distances the electrons only feel the outermost electron density variation at the edges of the conglomerates, which means that the efficiency is expected to be proportional to the ratio of the circumference to the area: $\eta \propto M^{-0.5}$.

In the case of semi-metals the scattering efficiency increases with the number of ad-atoms per cluster until the conglomerate radius exceeds the Fermi wavelength, Fig. 9. Then the efficiency decreases as in the metal case.

4. Summary

In the first part of this paper we gave an outline of our theoretical approach to surface roughness scattering. We presented a Fermi-Thomas like access to electronic screening of scattering potentials near a surface and derived simple formulas for the extra resistivity due to roughness scattering in which the surface profile autocorrelation plays the major role.

In the second part we discussed several types of autocorrelation functions. As examples for the high roughness regime we presented the results for a Gaussian, a Lorentzian and an exponential profile. For the submonolayer coverage we discussed the extra resistivity on one hand for isolated ad-atoms and on the other hand for the case of an island-like growth mechanism. With the aid of a scattering efficiency we showed that in the case of metals the conduction electrons are scattered only at the steps of the conglomerates. This concept can be applied to surfaces covered with several monolayers if the ad-atoms build laterally widely extended terraces. Here the case of deep roughness is included. The behaviour of semi-metals is characterized by their large Fermi wavelengths which leads to an enhanced scattering efficiency. This can be detected during an ad-layers growth from an overshooting of the extra resistivity in the Nordheim plot.

The authors are indebted to Prof. P. Grosse and Dr. D. Schumacher (University of Düsseldorf) for their interest in our work and their stimulating discussions.

References

1. Trivedi, N., Ashcroft, N.W.: Phys. Rev. B **38**, 12298 (1988)
2. Fuchs, K.: Proc. Camb. Phil. Soc. **34**, 100 (1938)

3. Wißmann, P.: The electrical resistivity of pure and gas covered metal films. Berlin, Heidelberg, New York: Springer 1975
4. Tellier, C.R., Tosser, A.J.: Size effects in thin films. Amsterdam, Oxford, New York: Elsevier 1982
5. Schumacher, D.: Surface scattering experiments with conduction electrons. Berlin, Heidelberg, New York: Springer 1993
6. Courths, R., Hüfner, S.: Phys. Lett. C **112**, 53 (1984)
7. Sambles, J.R.: Thin Solid Films **151**, 159 (1987)
8. Ziman, J.M.: Electrons and phonons. Oxford: Clarendon Press 1962
9. Soffer, S.B.: J. Appl. Phys. **38**, 1710 (1967)
10. Mayadas, A.F., Shatzkes, M.: Appl. Phys. Lett. **14**, 345 (1969)
11. Gerlach, E., Mycielski, J.: Verh. Dtsch. Phys. Ges. **17**, 746 (1982)
12. Gerlach, E., Mycielski, J.: (unpublished)
13. Gerlach, E.: Phys. Status Solid (b) **158**, 531 (1990)
14. Gerlach, E.: Phys. Status Solid (b) **157**, 189 (1990)
15. Gerlach, E., Kaser, A.: Phys. Status Solid (b) **167**, 233 (1991)
16. Hertling, R.: Diploma thesis. RWTH-Aachem 1993
17. Tešanović, Z. et al.: Phys. Rev. Lett. **57**, 2760 (1986)
18. Backes, W. et al.: Phys. Rev. B **45**, 8437 (1991)
19. Luo, E.Z. et al.: Phys. Rev. B **49**, 4858 (1994)
20. Pariset, C., Chauvineau, J.P.: Surf. Sci. **78**, 478 (1978)